Modelling turbulence intensity within a large offshore wind farm

Argyle, Peter; Watson, Simon; Montavon, Christiane; Jones, Ian; Smith, Megan

DOI
10.1002/we.2257

Publication date
2018

Document Version
Final published version

Published in
Wind Energy

Received: 19 November 2017 | Revised: 15 June 2018 | Accepted: 15 June 2018
DOI: 10.1002/we.2257

RESEARCH ARTICLE

WILEY

Modelling turbulence intensity within a large offshore wind farm

Peter Argyle[1] | Simon Watson[2] | Christiane Montavon[3] | Ian Jones[3] | Megan Smith[4]

[1] Loughborough University, CREST, Holywell Park, Ashby Road, Loughborough, UK
[2] TU Delft, Wind Energy Section, Aerospace Engineering, Delft 2629 HS, Netherlands
[3] ANSYS UK Ltd, Abingdon, UK
[4] The Carbon Trust, London, UK

Correspondence
Simon Watson, TU Delft, Wind Energy Section, Aerospace Engineering, Kluyverweg 1, Delft 2629 HS, Netherlands.
Email: s.j.watson@tudelft.nl

Funding information
Carbon Trust

Abstract

The IEC standard 61400-1 edition 3 uses the so-called Frandsen model to assess levels of turbulence intensity (TI) within wind farms, specifically to determine turbine suitability associated with stress and fatigue. Since the Frandsen model was developed, turbines have significantly grown in size and the number of turbines in an individual wind farm has grown in number. It is of interest to test the accuracy of such models, especially when applied to large wind farms offshore. This work presents results from comparing the Frandsen model with measured data from the Greater Gabbard offshore wind farm. Comparisons are also made with a simplified version of the Frandsen model. In general, both models were shown to perform well when predicting values of TI. However, the ambient wind farm turbulence model utilised by the Frandsen model was shown to be less reliable than the use of an individual turbine wake-generated turbulence model, regardless of distance, as demonstrated using a simplified model. The difference between observed mean and 90th percentile (also known as representative TI) values was in general larger than that predicted. It is proposed that this is primarily due to model reliance on variance in the turbulence of the freestream flow rather than actually modelling the variance of the turbulence generated by individual turbines, although this would require further work to confirm this.

KEYWORDS

Frandsen model, offshore wind farm, turbulence intensity

1 | INTRODUCTION

Modern wind turbines are commonly built as part of a large array. This means that individual machines will normally be in wake affected regions caused by other turbines, particularly for offshore locations where there are no obstacles or relief to dissipate these wakes. Such regions of increased turbulence intensity (TI), specifically high longitudinal variance (wind speed variation in the streamwise direction), increase the loads and fatigue on turbine blades[1] and significantly affect power curve measurements.[2] To help wind farm developers predict regions of elevated TI when designing wind farm layouts, the IEC Standard 61400-1 edition 3 amendment 1[3] describes the Frandsen model,[1] from which an effective turbulence intensity, I_{eff}, can be calculated. According to the standard, turbines are assessed as suitable for a site if the design TI is greater than the site effective TI, for wind speeds between 60% of rated and cut-out wind speeds. The effective TI is defined as

$$I_{eff}(U_0) = \left[\int_{-180}^{180} I^m f_{wd}(\theta|U_0)\,d\theta\right]^{\frac{1}{m}}, \quad I = \frac{\sigma(\theta, U_0)}{U_0}, \tag{1}$$

where m is the Wöhler exponent, θ is the wind direction, U_0 is the freestream wind speed at hub height, and f_{wd} is the fraction of the time the wind is coming from a particular direction θ, conditioned on the freestream wind speed U_0. It is important to stress that the turbulence intensity here is normalised to the *freestream wind speed* rather than the local wind speed at the position of interest, which is the more standard definition of TI. This definition means that the TI from the Frandsen model cannot be directly compared with a TI measured from local conditions within the wind farm. The Frandsen model was intended primarily as a way of assessing loads, and thus, σ (at a reference wind speed) is the main quantity of interest, together with the frequency distribution of the reference wind speed. The model is intended to be used with input data gathered *before* any wind farm is built and is therefore based on freestream mast measurements (ie, freestream wind speed). Therefore, in all comparisons made below, it is the freestream wind speed U_0 that is used in the denominator of I as stated in Equation (1).

For design purposes, the IEC Standard 61400-1 edition 3 amendment 1 stipulates that the effective TI should be calculated from the 90th centile value of the wind speed standard deviation, the so-called representative standard deviation σ_{repr}. The Frandsen model defines the *representative* value of $\sigma(\theta| U_0)$ as the standard deviation of the wind speed within a 10-minute period (sampled typically every 1-2 s) for a wind direction θ, which is thus dependent on location within the wind farm. Assuming a regular farm layout, this can be estimated depending on one of three cases:

$$\sigma_{repr,0} = \langle \sigma_0 \rangle + 1.28 stdev(\sigma_0), \tag{2}$$

$$\sigma_{repr,0,wf} = \langle \sigma_{0,wf} \rangle + 1.28 stdev(\sigma_0), \tag{3}$$

$$\sigma_{0,wake} = \sqrt{\frac{U_0^2}{\left(1.5 + 0.8\frac{d_i}{\sqrt{C_T}}\right)^2} + \sigma_{repr,0}^2}, \tag{4}$$

where σ_0 is the standard deviation of the freestream wind speed, $\langle .. \rangle$ represents the time-averaged value, C_T is the turbine thrust coefficient corresponding to the freestream wind speed U_0 (the Frandsen model assumes no change in wind speed within the wind farm), and d_i is the distance to the nearest upstream turbine, normalised by the turbine diameter.

Equation (2) is relevant when the location is assumed to be experiencing "freestream turbulence" (FT). In this case, $\sigma_{repr,\,0}$ is the representative wind speed standard deviation of the freestream flow and is considered valid up to the depth of five turbines into the farm for the corresponding wind direction, assuming the turbine separation is greater than 10 rotor diameters (D)—enough for turbine wakes to sufficiently dissipate. Equation (2) represents the 90th centile of the standard deviation of the freestream wind speed assuming σ_0 is normally distributed. The value calculated thus represents the turbulence level that is expected to be exceeded only 10% of the time.

Certain turbine wake models have shown the importance of boundary layer modification models when predicting wind speed reductions in large arrays,[4] and thus, the Frandsen model incorporates changes in boundary layer conditions for locations more than five turbines deep within the farm. This represents the second case, where the location of interest is assumed to be seeing "ambient wind farm turbulence" (WFT). For such locations, the 90th centile of the wind speed standard deviation is obtained from Equation (3), combining a mean wind farm standard deviation $\langle \sigma_{0,\,wf} \rangle$ with the standard deviation of the freestream wind speed standard deviation. The wind farm wind speed standard deviation $\sigma_{0,\,wf}$ is given by

$$\sigma_{0,wf} = \frac{1}{2}\left(\sqrt{\sigma_{add,wf}^2 + \sigma_0^2} + \sigma_0\right), \tag{5}$$

where

$$\sigma_{add,wf} = \frac{0.36 U_0}{1 + 0.2\sqrt{s_f s_r / C_T}} \tag{6}$$

and s_f and s_r are the distances between neighbouring turbines in the same streamwise row and lateral row, respectively; each of which has been normalised by the rotor diameter.

In some instances, the turbulence generated by a single local turbine may be more significant than the overall effect of the farm at a particular location of interest. Thus, the Frandsen model specifies a third case, namely, a "wake turbulence" (WT) described in Equation (4), which applies for a location and direction when a turbine is less than 10D away in that direction.

The Frandsen model values of $\sigma(\theta| U_0)$ as defined by Equations (2), (3), and (4) indicate the 90th centile of the normally distributed turbulence; this investigation will also consider the *mean value* of the distribution by substituting the following three equations where appropriate:

$$\sigma_{mean,0} = \langle \sigma_0 \rangle, \tag{7}$$

$$\sigma_{mean,0,wf} = \langle \sigma_{0,wf} \rangle, \tag{8}$$

$$\sigma_{0,wake} = \sqrt{\frac{U_0^2}{\left(1.5 + 0.8\frac{d_i}{\sqrt{C_T}}\right)^2} + \sigma_{mean,0}^2}. \tag{9}$$

Since turbine wakes are known to both horizontally meander and expand,[5] a function is required for determining which directions are in the wake of each turbine. The IEC standard[3] indicates following Figure 1 that for regular arrays, the wake contribution from eight neighbouring turbines should be considered in making a calculation of the resulting effective TI at a turbine within the array. For irregular arrays, however, the main turbulence contributing turbines is open to interpretation although it has been suggested[6] that with sufficient care, the rule can still apply. Although Jacquemin et al[6] compared two different well-established methods for calculating the view angle (θ_w) with values varying by 10% to 70% depending on the wake decay factor used, it was suggested that the method may not be important as any difference in TI tended to be governed by the ambient turbulence correction within a large farm. This paper uses the definition of θ_w used by Frandsen[1] shown in Equation (10) where θ_w is always at least 15° for turbine separations less than 10D:

$$\theta_w = \left(\tan^{-1}\frac{1}{d_i} + 10^{\circ}\right). \tag{10}$$

As Equation (10) leads to larger values of θ_w at close distances, some directions will be within the view angle of multiple turbines—even though they are not directly aligned. In such cases, the TI generated by the closer turbine takes priority whilst the further turbine is ignored.

The wind farm–added TI is based on the assumption that TI generated by the wind farm can be superimposed on top of the freestream TI. The validity of this assumption is beyond the scope of this paper. Using the assumption that an infinite array effectively increases the surface roughness, the wind profile above hub height is modelled by a log profile with increased roughness and friction velocity. This modified roughness regime requires the turbines to be within the atmospheric surface layer (which they might not be under stable atmospheric conditions) and is only truly valid above the top of the rotor tips rather than at hub height. Since the Frandsen model was developed using data from turbines much smaller than modern machines, these assumptions may no longer be as reliable.

The purpose of this work, therefore, is to assess how well the Frandsen model performs at the locations of several individual turbines and two meteorological masts within a large operational offshore wind farm where the distance to neighbouring turbines, as a function of direction, varies within a wide range. Specifically, we compare mean and representative TI values predicted by the Frandsen model both against measured values and against values predicted by a "Simplified" model. This Simplified model utilises Equations (4) and (9) to calculate σ when a turbine is within the view angle at the location of interest regardless of distance, whereas Equations (2) and (7) are used for directions without any turbines upstream, ie, the Simplified model makes no assumption of an "ambient WFT" beyond an arbitrary distance (10D in the case of the Frandsen model). It should be stressed that no *new* model has been developed as part of this work, rather we assess a simplified implementation of the existing Frandsen model. In addition, it should be pointed out that the Frandsen model is a conservative model whose principal purpose is for making fatigue calculations. This work makes no assessment as to the suitability of the model for this purpose but merely assesses its overall accuracy in predicting levels of turbulence intensity.

The next section reviews past work to compare wake models with measured WFT intensity. This is followed by a description of the Greater Gabbard site used for this study. The section that follows this provides a detailed analysis of the measured data and the comparisons with both the Frandsen and Simplified Model. The paper then concludes with some summary observations based on the analysis.

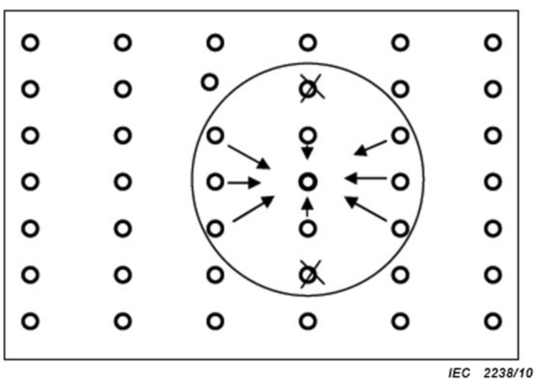

FIGURE 1 Schematic showing the turbines (small circles with arrows) contributing to the direct wake contribution in the effective TI for the turbine in the centre of the large circle (source: IEC standard 64100-1, Ed 3, amendment 1). Turbines outside the large circle or with crosses through them are assumed not to contribute to the direct wake

2 | PREVIOUS VALIDATION OF WAKE MODELS FOR PREDICTING TURBULENCE INTENSITY

Although there has been much research to develop wake models in order to predict reductions in wind speed and thus power output in wind farm arrays, there has been little work to develop models with the aim of predicting turbulence intensity. Indeed, the aim of the Frandsen model was primarily to determine levels of loading on machines rather than to develop a stand-alone model for turbulence intensity. There have been few studies to consider how well semiempirical models such as that developed by Frandsen perform in the field. Such models have generally been calibrated using measurements behind a full-scale turbine or from large eddy simulation model results and have only been developed and tested for the prediction of turbulence intensity behind single turbines.[7,8]

Frandsen and Madsen introduced the concept of WFT during a study of the Nørrekær Enge II wind farm.[9] They showed that from measurements above rotor height, there was a good correspondence between the measurements and a WFT model that was to form part of the methodology described in the introduction above. The authors did note caution in interpreting the results given the position of the meteorological mast used for the measurements. A comparison was made between turbulence intensity predicted by a so-called "Windfarm Assessment Tool" based on Frandsen's wake–added turbulence intensity expression in the IEC 61400 standard and data from the Middelgrunden offshore wind farm consisting of a single row of machines aligned in a gentle curve.[10] This showed relatively good agreement with the trend, although absolute values were underestimated. This was attributed to the fact that the ambient level of turbulence intensity assumed by the Windfarm Assessment Tool model neglected the effects of stability and the fact that the site was so close to land. Measurements were made down a line of five 2.5MW wind turbines at the Wieringermeer test site run by ECN in the Netherlands. A comparison was made between models and measurements of velocity deficit and wind speed standard deviation.[11] It was assumed that the variance of the freestream wind speed, σ_0^2, could simply be added to the variance of the wind speed generated by a turbine, σ_{rotor}^2, to give the total variance of the wind speed, σ_{total}^2, measured downstream of a turbine:

$$\sigma_{total}^2 = \sigma_0^2 + \sigma_{rotor}^2. \tag{11}$$

The model for added wind speed standard deviation consisted of a power law decaying function downstream of the rotor and two Gaussian type peaks originating from the edges of rotor in the span-wise direction that merge eight diameters downstream of the rotor. The initial level of added standard deviation was based on the thrust on the rotor from the Gunner C. Larsen GCL model.[12] The results showed a significant underprediction of the measured standard deviation that was attributed to several factors: no account taken of added turbulence from the nacelle, no account taken of the effect of freestream ambient turbulence intensity on the decay of added turbulence, and the fact that the model parameters did not correctly model the decay of wake added turbulence.

Wind tunnel experiments with model turbines considered the variation in turbulence intensity with a regular aligned array of 10 × 3 turbines.[13] It was found that turbulence intensity increased for the first three or four rows of turbines and plateaued from around the fifth row, which would seem to confirm the Frandsen model approach of using an ambient WFT when more than five turbines into a wind farm. Similar experiments in the same wind tunnel but with a staggered array[14] showed that the maximum levels of turbulence intensity did not increase significantly beyond the first row that was partly attributed to the fact that the wake from an upstream turbine had twice as long to recover compared with the aligned case. Further comparisons were made between aligned and staggered arrays.[15] The turbulence intensity at hub height behind the eleventh row of turbines, taken as representative of wind farm–added turbulence intensity, showed good agreement between experimental values and those calculated using Equation (6) for both aligned and staggered configurations (values were very similar for both configurations) given uncertainties in determining the experimental thrust coefficients.

A study using rotor effective wind speed[16] showed that for the Lillgrund offshore windfarm when analysing wind directions with a 3.3D effective spacing, levels of turbulence intensity increased significantly for the first two rows of turbines but there was no real increase beyond this; however, for Horns Rev I for directions with an effective 7D spacing, levels of turbulence intensity increased up to around five rows into the wind farm. This would partly seem to agree with the guidelines of the Frandsen model that suggests that turbine spacing is relevant when considering how far into the wind farm one needs to be before wakes have sufficiently diffused to result in an overall wind farm background turbulence intensity level.

There has been work to compare the Frandsen model with computational fluid dynamics (CFD) simulations of a wind farm. A comparison was made between large eddy simulations of 16 turbines in the streamwise direction, using boundary conditions to effectively make the wind farm infinitely wide in the lateral direction.[17] Comparisons were made between the Frandsen model and simulations for a range of freestream wind speeds and turbulence intensities. It was shown that the Frandsen model performed well in general but was conservative as expected. Far WT intensity was well predicted, although the blockage effect of the rotors meant that turbulence intensity immediately in front of each rotor was overestimated.

The Dynamic Wake Meander model was developed to superimpose meandering due to atmospheric turbulent eddies on top of quasi-static wakes and incorporate wake-generated turbulence. This model has been validated against observed data and CFD simulated data including Egmond aan Zee.[18] Good agreement was noted for both observed power production and turbine loading although there was no direct comparison between predicted and measured turbulence intensity.

The foregoing review shows that what little work there has been to date on developing and validating large WFT intensity models has used limited data from a few mostly modest-sized wind farms, wind tunnel experiments, or CFD model simulations. In this work, we analyse turbulence intensity within a large offshore wind farm and endeavour to gain an insight into the accuracy of the Frandsen model when used in the context of a large array.

3 | SITE DESCRIPTION

This work uses measurements from the Greater Gabbard wind farm situated in the North Sea (see Figure 2), consisting of Siemens 3.6MW turbines (h_{hub} = 77.5 m, D = 107 m) with a layout as shown in Figure 3. The turbines have power and thrust coefficient curves as shown in Figure 4. The farm consists of two subarrays: a northerly section that has 102 turbines and a southerly section with 38. Typical turbine separations within the near-regular array are ~9.7D (200°), ~10D (247°), and ~8.3D (315°) whilst the shortest distance between the two subarrays is 73D. There are two masts providing meteorological data: IGMMZ is embedded within the northerly section whilst mast IGMMX is located on the southerly edge of the northern subarray, just 2.46D away from turbine IGF10. As the layout of the turbines in the Greater Gabbard wind farm is not fully regular, average values of s_f and s_r have been calculated for use in Equation (6). The value of s_f was calculated as the overall average between neighbouring turbines in the same row, whilst s_r was calculated by dividing the separation between IGB05 and IGL01 by the number of rows in between them, ie, 10. This resulted in values of 8.96D and 7.66D for s_f and s_r, respectively.

4 | ANALYSIS

4.1 | Freestream conditions

Although there are two met masts at the Greater Gabbard site, they are both located downstream of wind turbines for most of the directions, with only partial access to atmospheric freestream conditions. Therefore, a "Freestream" dataset has been generated using the nacelle anemometry from six turbines located at prominent locations on the edge of the farm, when they are yawed away from upstream turbines. The wind direction was taken as the average of the six turbines to minimise the effect of any directional offset. As will be shown later in this paper, there is a good correspondence between the directions of the peaks in observed TI and the bearings of the closest turbines that gives some confidence that the direction inferred from the average of the nacelle wind vanes is accurate. The six turbines used to infer the freestream conditions are shown as open circles in Figure 3, along with the resulting hub height wind rose (at 10 ms^{-1}) and hub height wind speed frequencies. The physical structure of the turbine nacelle will likely alter the wind flow in addition to the effects of the rotating turbine blades. To attempt to correct for this, a linear calibration was calculated by correlating hub height measurements from the southerly met mast IGMMX with measurements from the nacelle of the nearest turbine IGF10, 2.46D away. Figure 5 shows how the wind speed measurements differ between mast- and nacelle-based instrumentation. If it is assumed that a met mast measures the "true" conditions, then the nacelle-mounted anemometer shows a very good correlation with

FIGURE 2 Site of the Greater Gabbard offshore wind farm off the east coast of the UK. Courtesy of Google Earth [Colour figure can be viewed at wileyonlinelibrary.com]

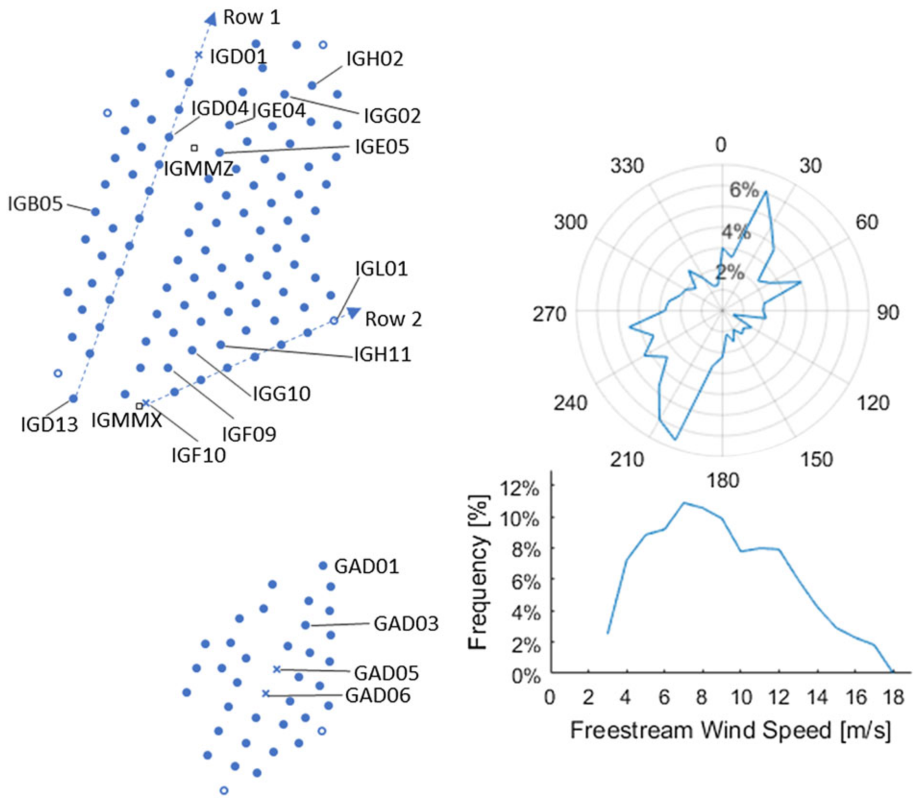

FIGURE 3 Left: The Greater Gabbard wind farm layout with the met masts IGMMZ (northerly) and IGMMX (southerly) shown as black squares, open circles are the six turbines used to calculate the freestream wind conditions whilst labelled crosses (IGD01, IGF10, GAD05, and GAD06) show the turbine locations where turbulence intensity was investigated in this work. All other turbines are shown as solid circles. A number of other turbines are labelled, which are referred to later in this paper. Rows 1 and 2 are the two rows of turbines along, which the variation of turbulence intensity was investigated. Right Top: The wind rose at hub height for the wind farm generated from the freestream dataset at 10 ms^{-1} at 10° resolution. Right Bottom: The wind speed frequency distribution at hub height determined from the freestream dataset at 1-ms^{-1} resolution [Colour figure can be viewed at wileyonlinelibrary.com]

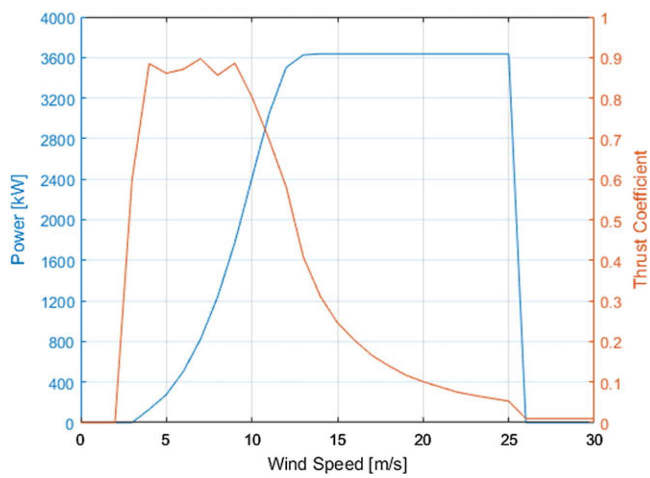

FIGURE 4 Power (blue) and thrust coefficient (red) curves for the Siemens 3.6MW turbines at Greater Gabbard [Colour figure can be viewed at wileyonlinelibrary.com]

the "true" wind speed (Figure 5A) although the slope is less than one and there is a positive offset. By contrast, the correlation of the mast and turbine standard deviation within each 10-minute interval (Figure 5B) is lower than for the mean wind speed with a slope greater than one and a small negative offset. This might be expected due to turbulence added by the nacelle and blades. However, it can be seen in Figure 5C that there is a cut-off in measured standard deviation particularly at low wind speeds and some evidence of aliasing of the values. This is due to the finite frequency response of the cup anemometer at low rotational (sampling) speeds. In the absence of this effect, the slope of the line in Figure 5B would be closer to 1. It can also be seen in Figure 5D that there is significant variation in the ratio between the standard deviation recorded on the nacelle and that on the mast when considered as a function of wind speed. The distribution of the ratio reflects the operational point

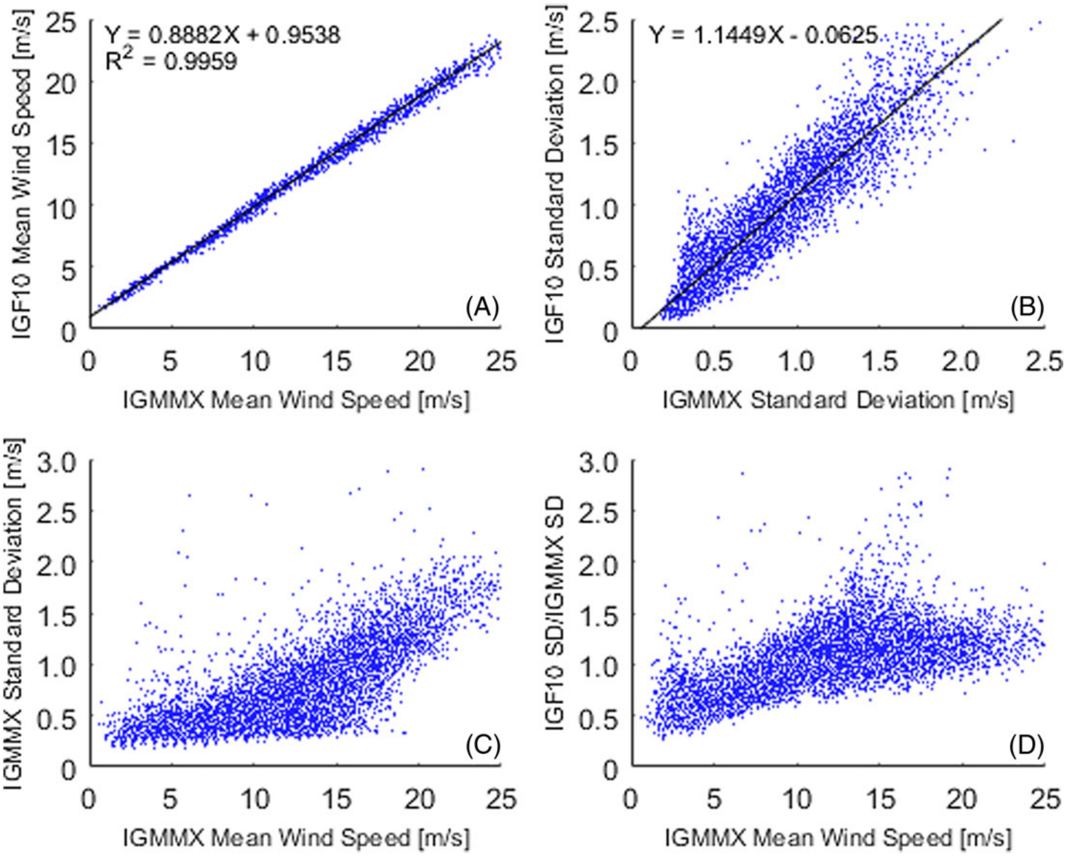

FIGURE 5 The measurement offset between the cup anemometers located on mast IGMMX and turbine IGF10. A, Ten-minute mean wind speed; B, 10-minute wind speed standard deviation, C, ratio of wind speed standard deviation measurements by mean wind speed, D, relationship between wind speed mean and standard deviation measurements at met mast IGMMX. Note that (C) shows a cut-off and evidence of aliasing of the measured values for wind speeds between 5 and 10 m/s and low values of standard deviation [Colour figure can be viewed at wileyonlinelibrary.com]

on the turbine thrust curve and thus the turbulence created by the blade rotation and pitching. Once the turbine starts to regulate around 9 to 10 m/s, this ratio is close to one, although the largest scatter occurs when the turbine switches above and below rated output.

By defining the freestream as the average of turbines spread over a large area, it is assumed that the variation across the wind farm area is small and does not change rapidly with time. It is acknowledged that there can be significant variation in certain circumstances, eg, where there is a blockage effect imposed by the wind farm or where the wind farm is relatively close to land and the distance from the coast varies across the wind farm. However, the intention of this work was to test the accuracy of the Frandsen model, which assumes a constant freestream wind speed within the wind farm, thus averaging over turbines was considered a reasonable approach. It should be noted that the calibration used here to convert nacelle measurements to mast equivalents is likely to vary between wind farms as it will be dependent on the turbines used. Indeed, the required calibration may even vary between turbines within the same farm, although the farm layout at Greater Gabbard makes this hard to corroborate, leading us to assume a constant calibration across the whole farm.

4.2 | Turbulence intensity at specific wind farm locations

In this paper, the applicability of the Frandsen model for predicting turbulence intensity at the locations of the two meteorological masts and several operational wind turbines in the Greater Gabbard offshore wind farm is considered. The meteorological masts, IGMMX and IGMMZ, are marked as open squares in Figure 3. The turbines investigated (shown as crosses in Figure 3) are IGD01, IGF10, GAD05, and GAD06 and have been selected for different reasons. Turbine IGD01 is located at the northern end of 13 turbines closely aligned to the prevailing south-westerly wind, and so analysing results from this turbine will test the validity of Equations (3) and (4). By comparison, turbine IGF10 is located on the southern edge of the northern subarray and is well positioned to investigate wake effects from both the frequent north-easterly direction and any wake shadow from the southerly subarray. The proximity of turbine IGF10 to mast IGMMX is also useful for validating the accuracy of Equation (4) under near-wake conditions. Turbines GAD05 and GAD06 are located centrally in the southerly array and allow a comparison of the standard Frandsen and Simplified models in a smaller array as well as allowing an analysis of how TI varies down a line of turbines. In order to visualise the proximity of the two masts and the four chosen turbines to the other turbines in the wind farm, distances as a function of bearing are shown in Figure 6. Distances are normalised to rotor diameter (D) and plotted on a reverse logarithmic scale to emphasise the closest turbines, which will

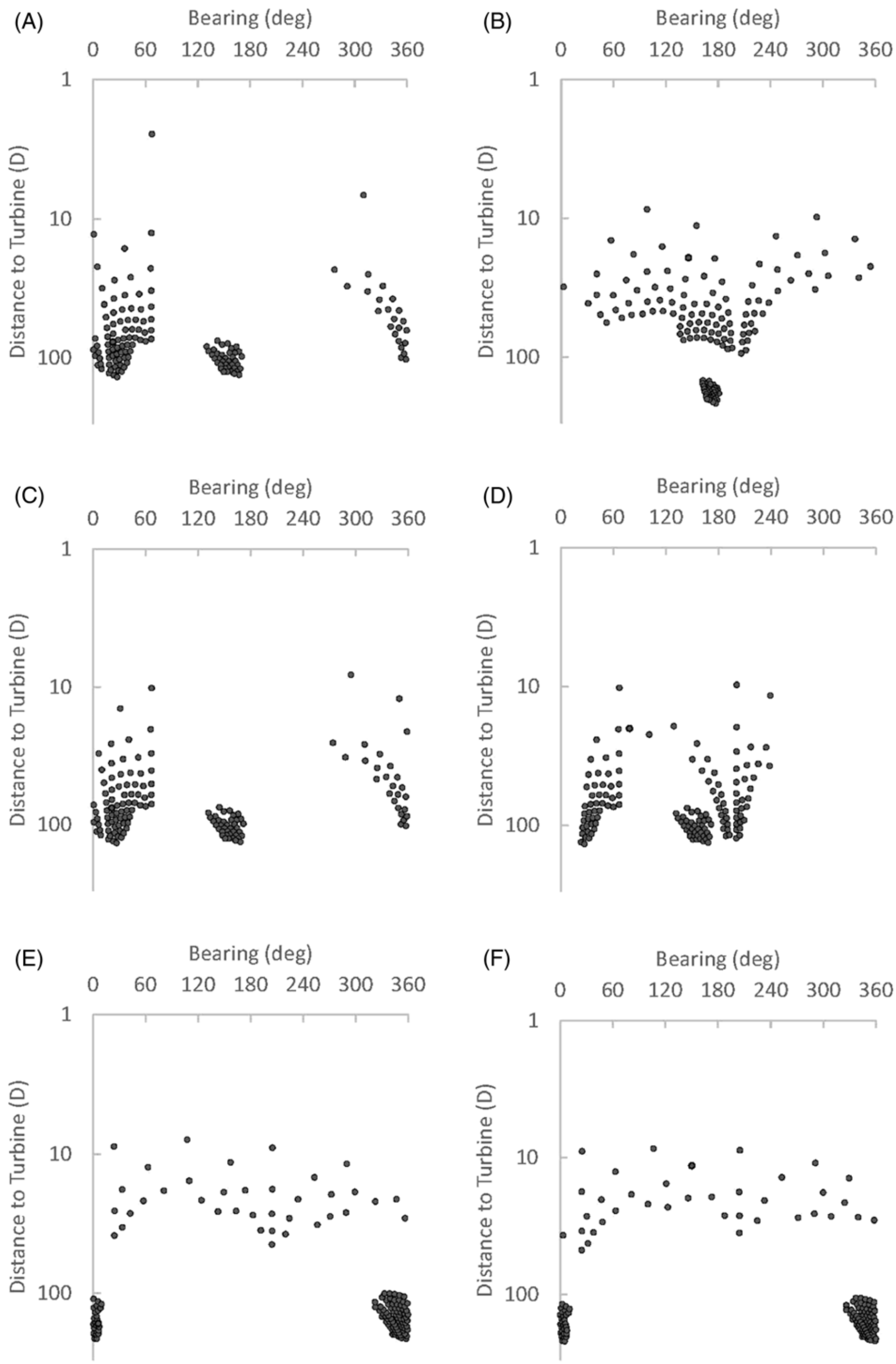

FIGURE 6 Turbine distances as a function of directional bearing for A, IGMMX; B, IGMMZ; C, IGF10; D, IGD01; E, GAD05; and F, GAD06

have proportionately the greatest effect on turbulence intensity. It can be seen that most of the turbines are more than 10D away for the six locations; however, there are a few cases where turbines are closer than or around 10D. This gives an opportunity to assess the performance of the Frandsen model at a range of distances.

In the following analysis, the mean and representative values of TI averaged by 10° sector are calculated using the Frandsen and Simplified Models (from Equations (2) to (10)) for a freestream wind speed of $10 \pm 0.5\ \mathrm{ms^{-1}}$ based on the appropriate freestream turbines described above. The value of $10\ \mathrm{ms^{-1}}$ was chosen as this represents the case where wake effects are likely to be significant. The results are compared with the measured values. The individual values of TI were calculated using mean freestream wind speeds and turbine local standard deviation values corresponding to each 10-minute event. In the following figures, both the 10° sector-averaged measured values (marked as large black dots) and the individual 10-minute events (marked as smaller grey dots) are shown. This was done to indicate the spread of measured values about their mean.

Figure 7 shows results from mast IGMMX located on the edge of the northern array. The two largest peaks correspond well with two closest turbines shown in Figure 6A. In this case, the Frandsen model returns mean TI values similar to those measured but tends to overestimate the main

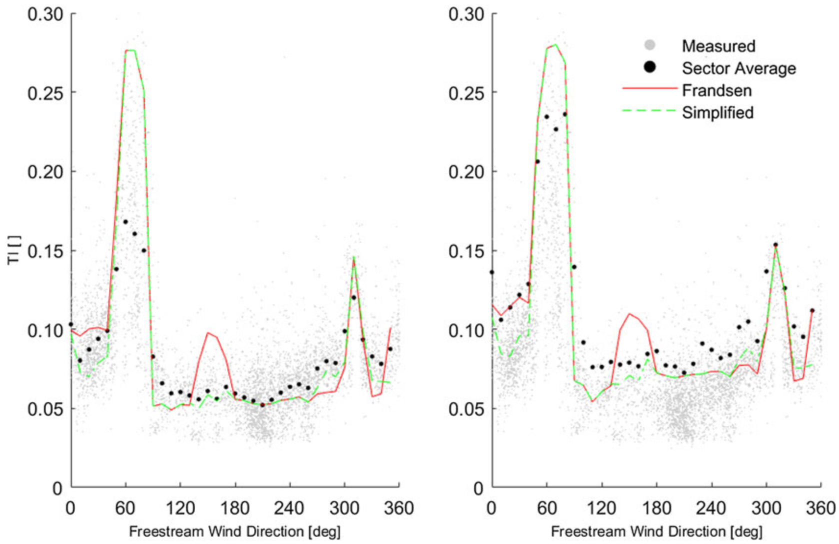

FIGURE 7 Mean (left) and representative (right) values of TI for the southern met mast IGMMX for a 10-ms^{-1} freestream wind speed. Note: Small grey dots (measured) represent individual 10-minute events, large black dots (sector average) represent 10° sector averages [Colour figure can be viewed at wileyonlinelibrary.com]

peaks and underestimate the mean TI for the sectors in-between the peaks. It also produces an artificial peak between the sectors 140° to 170° as a direct result of the southern array being large enough to generate the wind farm internal boundary layer required for WFT and being considered part of the same farm despite being located far enough away for significant wake recovery. In a lot of sectors, the Frandsen model underestimates the mean TI as there are less than the required five turbines upstream to trigger the use of WFT and for the less than five that are upstream; most are beyond the 10D cut-off point for WT. In both these cases, the Simplified model performs better in predicting the mean TI as it acknowledges that whilst the turbines upstream generate additional turbulence, it also allows for this additional turbulence to dissipate with distance although possibly too quickly.

When looking at the representative TI, both the Frandsen and Simplified model still overestimate the main peak for the sectors 60° to 70° but provide a good prediction of the peak for the sector 310°. Whilst the Simplified model does not produce the excessively large peak associated with the southern array for the sectors 140° to 170°, it does not provide a real improvement in modelling the representative TI between the main peaks, often underestimating the measured values.

The significant overestimation around the sectors 60° to 70° is likely a consequence of the fact that the Frandsen model was not designed or calibrated for the near wake region. The model assumptions do not allow the model to capture any fine structure in the wake development, which are likely to affect the measurements at a distance of 2.46 rotor diameters. For the near wake peak around the sectors 60° to 70°, it is noticeable that there is a large difference between the measured mean and representative TI, indicating that the standard deviation of the wind speed standard deviation is large. This is not captured by the model, either because the mean TI predicted in the near wake is excessive, or because the variability of the turbulence in the wake region is not accounted for (or a combination of both). Note that in the case of both models, the freestream TI derived from the turbines tends to underestimate that measured at mast IGMMX for certain directions. This is noticeable between 230° and 260°. The reasons for this are unclear; however, it may be that the calibration derived using IGF10 and IGMMX is not accurate for all of the six turbines used to estimate the freestream conditions.

Figure 8 shows the results from mast IGMMZ deep within the wind farm. There are peaks corresponding well to the six closest turbines seen in Figure 6B, although the peak at 155° is lower than might be expected given the turbine separation for reasons explained below. Unsurprisingly,

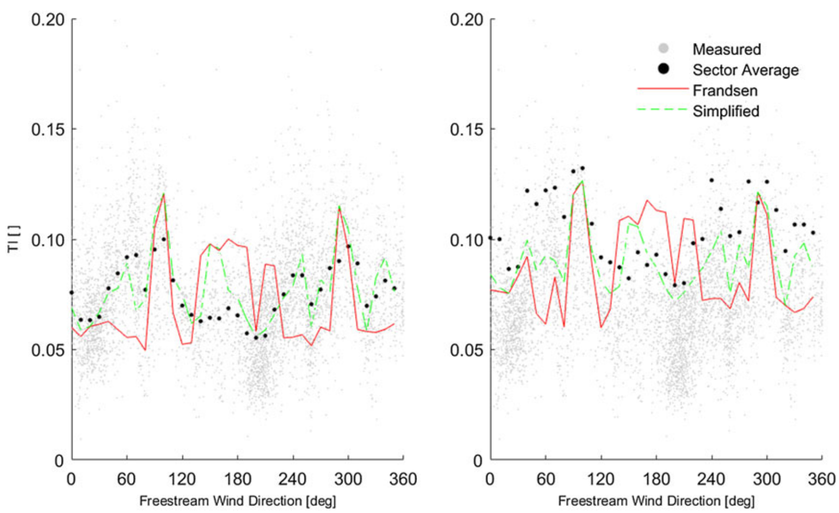

FIGURE 8 Mean (left) and representative (right) values of TI for the northern met mast IGMMZ for a 10-ms^{-1} freestream wind speed. Note: Small grey dots (measured) represent individual 10-minute events, large black dots (sector average) represent 10° sector averages [Colour figure can be viewed at wileyonlinelibrary.com]

the distribution of TI by direction is much more complex here, although the Simplified model predicts the mean TI well and more consistently than the Frandsen model. It should be noted that there was significantly reduced availability for turbine IGE06 located 11.3D upstream in the sectors 150° to 160°, which led to the measured TI being lower than predicted. The Frandsen model struggles to capture the mean TI at mast IGMMZ, underestimating where there are too few turbines to trigger the use of WFT and often overestimating in the cases where there are sufficient upstream turbines to justify its use. Directions when the Frandsen model is most accurate correspond to the only two cases where turbines are within 10D distance—IGE05 and IGD04 at sectors 100° and 290°, respectively—and directions parallel to the main gap (sector ~200°) in the northerly array, which is roughly 17D wide. Both models struggle to capture the standard deviation of the turbulence and thus underestimate the representative TI, most likely due to Equation (4) only accounting for the variance in the FT rather than any variability in turbulence generated by direct wake effects as mentioned above.

The results for the TI at turbine IGF10 are shown in Figure 9. In this case, the four most prominent observed peaks correspond well to the closest four turbines as shown in Figure 5C. This turbine is very close to IGMMX and thus would be expected to experience similar levels of turbulence to the met mast from the wakes resulting from the two turbines at bearings of around 290° and 350°. However, the nearest turbine along the line of machines at a bearing of around 70° is much further away (just over 10D) than the equivalent turbine seen by IGMMX (IGF10 itself). Indeed, the TI peak in Figure 7 due to IGF10 is significantly greater than the equivalent peak at 70° seen in Figure 9. This is worth noting as the increased distance is beyond the arbitrary cut-off distance used by the Frandsen model for the validity of WT, resulting in a significant under-estimation of TI by the Frandsen model whilst the Simplified model with no such cut-off performs better. Both models again fail to quantify the increase in TI due to the southern array, with the Frandsen model significantly overpredicting it and the Simplified model slightly under-predicting the representative TI but succeeding with the mean TI values. There is little difference in TI values for the more northerly directions although it is notable that the representative TI around 290° is modelled well in both cases.

In Figure 9, for IGD01, we would expect to see three main peaks in TI at 67°, 201°, and 240° when referring to the closest turbines shown in Figure 6D. The latter two are prominent, although the former is less obvious, but still visible. Since turbine IGD01 is located on the northern edge of the farm, it is logical to expect Figure 10 to show increased TI in the opposite directions to Figure 9. Despite there being no upstream obstructions for a broad sector around the northerly direction (260° to 60°), both the models slightly underestimate mean and representative TI for this sector. As both models determine TI using FT for this freestream sector, it is unsurprising that their results are identical; however, that they return values lower than measured on the turbine nacelle suggests that the discrepancy may come from differences between the values of $\sigma(\theta| U_0)$ as measured on the nacelle of turbine IGD01 and the freestream dataset. In this case, the IGD01 values of $\sigma(\theta| U_0)$ are higher than their freestream counterparts, yet since the freestream values were also acquired from nacelle anemometry, it is unlikely the blades on IGD01 cause significantly more turbulence than the other turbines in the wind farm. Thus, the discrepancy most likely stems from variations within the freestream flow across the width of the wind farm between the turbines used to calculate the freestream flow conditions. Indeed, this may also be further evidence that the calibration applied to the standard deviation shows variation between turbines. Figure 5 shows that there is a significant degree of scatter between mast and nacelle measured TI. This highlights the importance of obtaining a reliable freestream dataset, and model results may improve if more turbines had been included from the centre of freestream-facing farm edges.

Positioned at the downwind end of 13 turbines aligned with the prevailing wind, with most turbines separated by just less than 10D, WT used by both models captures well the representative TI spike at 200°. WT also captures the spike at 240° caused by three turbines as shown by the

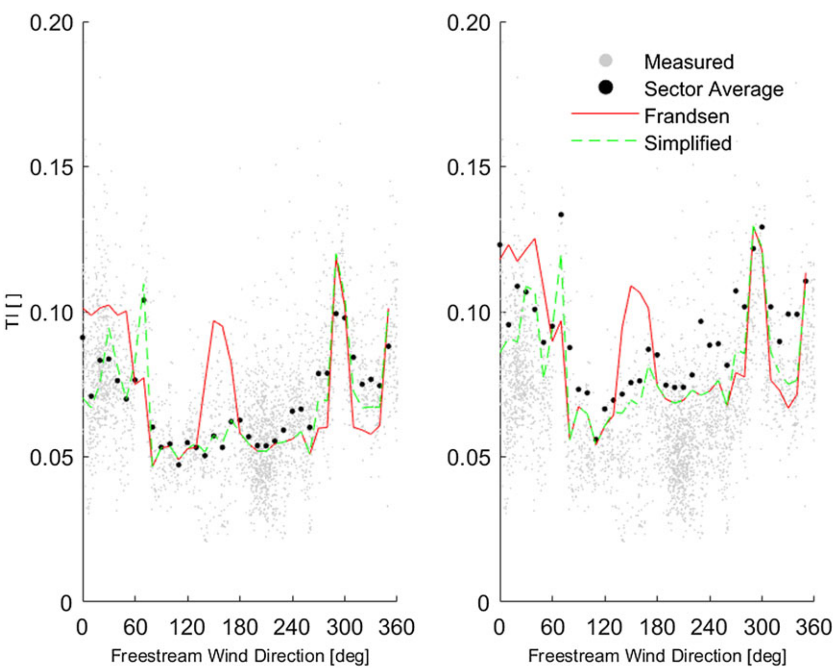

FIGURE 9 Mean (left) and representative (right) values of TI for the turbine IGF10 for a 10-ms^{-1} freestream wind speed. Note: Small grey dots (measured) represent individual 10-minute events, large black dots (sector average) represent 10° sector averages [Colour figure can be viewed at wileyonlinelibrary.com]

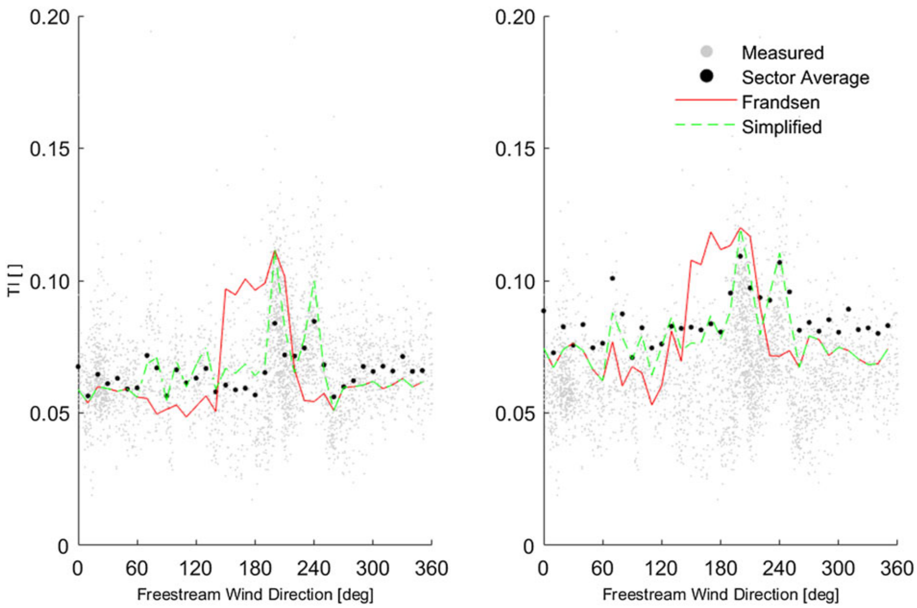

FIGURE 10 Mean (left) and representative (right) values of TI for the turbine IGD01 for a 10-ms^{-1} freestream wind speed. Note: Small grey dots (measured) represent individual 10-minute events, large black dots (sector average) represent 10° sector averages [Colour figure can be viewed at wileyonlinelibrary.com]

Simplified model whilst due to the nearest turbine being located 12D upstream, the Frandsen model assumes freestream conditions and thus misses the spike. Also, very clear is the sector between 150° to 210°, which contains enough turbines for the Frandsen model to use WFT, resulting in a significant overprediction of both mean and representative TI. Again, the results from the Simplified model using WT perform better between 70° and 140° than the Frandsen model, which uses FT in this sector.

Figures 11 and 12 compare the TI values for turbines GAD05 and GAD06, respectively, located in the middle of the southern array. These were chosen to be next to each other to determine whether the conditions at the turbines were similar. It can be seen that this was indeed the case. From Figure 6E,F, it might be expected to see peaks from seven or eight closest turbines around or just closer than 10D. The peaks do seem to correspond to these turbines, although there is some scatter in the mean observed values. As with the previous locations, the modelled values of TI in direct wakes overestimate mean values but generally provide an underestimate of the standard deviation, resulting in an underestimation of the representative TI. This is particularly noticeable in sectors 220° to 270°. For the northerly sector influenced by the larger turbine array, the Frandsen model overestimates the mean TI using WFT whilst the Simplified model is more accurate using WT. This is possibly because despite there being plenty of turbines upstream, there is a larger than normal gap between turbines upstream of GAD05 as well as the ~70D gap between the northern and southern array where TI can dissipate. The two most prominent spikes in TI for both figures occur around 25° and 205°,

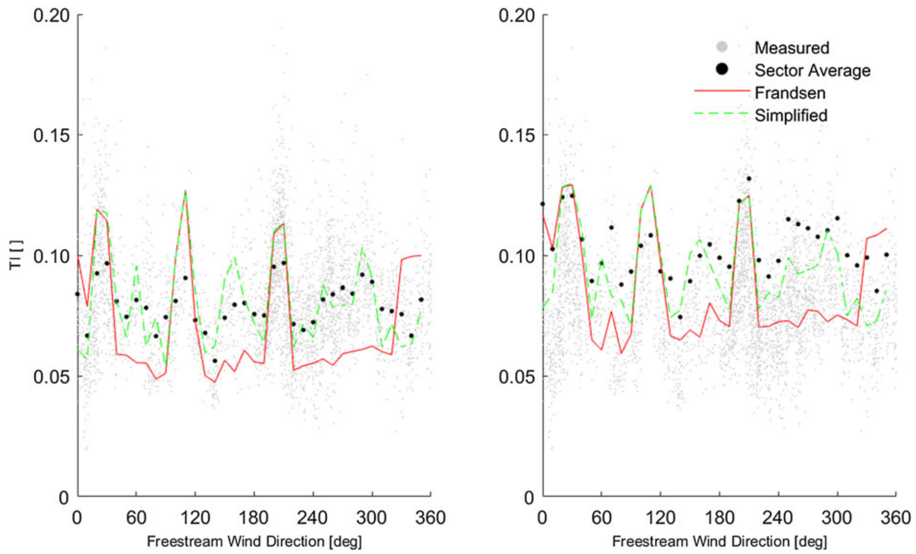

FIGURE 11 Mean (left) and representative (right) values of TI for the turbine GAD05 for a 10-ms^{-1} freestream wind speed. Note: Small grey dots (measured) represent individual 10-minute events, large black dots (sector average) represent 10° sector averages [Colour figure can be viewed at wileyonlinelibrary.com]

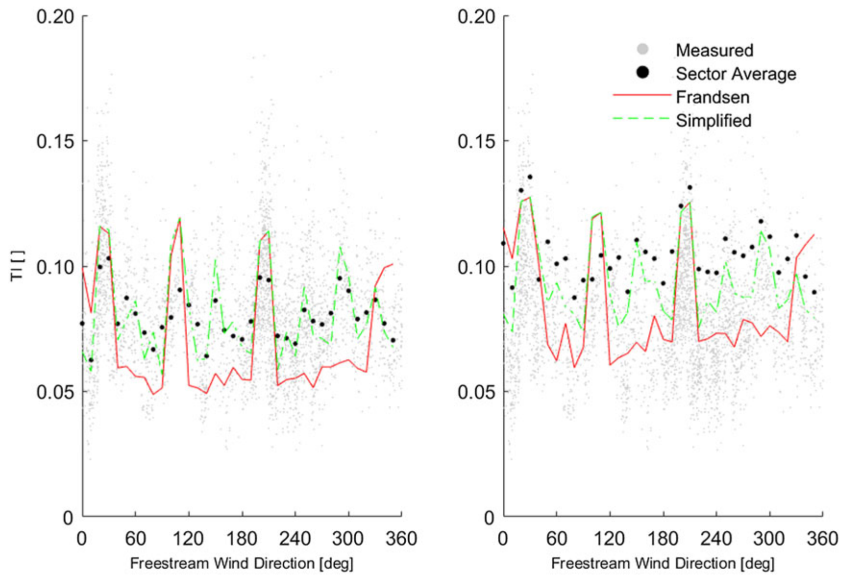

FIGURE 12 Mean (left) and representative (right) values of TI for the turbine GAD06 for a 10-ms^{-1} freestream wind speed. Note: Small grey dots (measured) represent individual 10-minute events, large black dots (sector average) represent 10° sector averages [Colour figure can be viewed at wileyonlinelibrary.com]

the directional alignment of the two turbines within the row. There is a slightly smaller third peak due a close turbine at a bearing of around 110°. There is little discernible difference between the TI measurements at the turbines for the 205° sector but turbine GAD06 measures slightly more TI for directions around 25°. It should be noted that along the row, there are nominally four turbines in front of GAD05 aligned around the 25° bearing and five turbines in front of GAD06 aligned around the 205° bearing; however, the locations of turbines GAD01 and GAD03 situated to the north-east of the subarray do not conform to the farm uniformity. Turbine GAD03 is 9° out of line whilst turbine GAD01 is separated an additional 4D further than the other turbine separations within the row. Whilst the modelled TI is dependent on both the neighbouring turbines conforming to the regular array layout (turbine separation here is less than 10D), and any variations in the freestream flow, the measured TI is also affected by turbine wakes between the edge of the farm and turbine directly upstream. Both of these factors contribute to the measured representative TI for the 25° sector for turbine GAD05 being lower than modelled in contrast to turbine GAD06 where the measured representative TI is higher than modelled for the 205° sector.

4.3 | Turbulence intensity variation with turbine distance

In the figures presented above, TI was shown by direction. Whilst this helps with generating a picture of what conditions are like at specific locations by direction in relation to the farm layout for Greater Gabbard, it is hard to assess how well each model performs with distance from the turbulence source and whether an arbitrary condition on turbine separation is suitable for determining the TI calculation method. To try and provide further insight into the performance of the models in general, Figure 13 shows the mean TI values using σ data measured at both

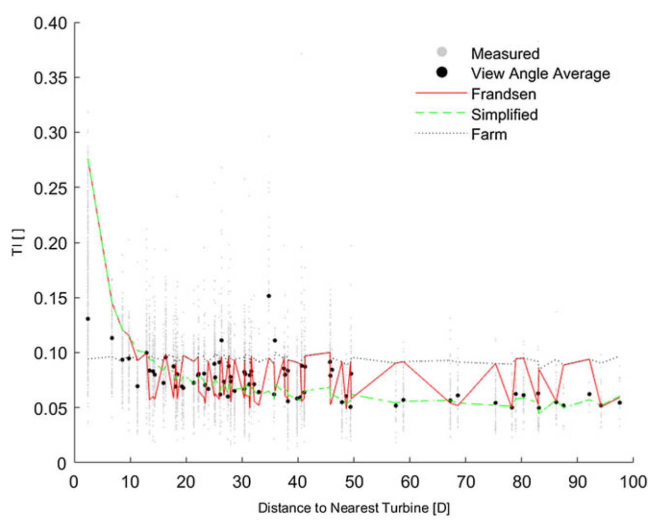

FIGURE 13 Mean TI measured at and modelled for both masts as a function of the distance between mast and the nearest wake-producing turbine upstream, as determined by the view angle, for any given direction and 10-m/s mean freestream wind speed. Note: Small grey dots (measured) represent individual 10-minute events, large black dots (view angle average) represent averages over the view angle for the wake-producing turbine [Colour figure can be viewed at wileyonlinelibrary.com]

masts IGMMX and IGMMZ alongside values predicted by the Frandsen and Simplified models against the distance to the nearest wake-producing turbine for any given freestream wind direction. The mast is deemed to be experiencing wake-generated turbulence from a particular turbine if that turbine for a given direction is within the view angle defined in Equation (10). For reference, the predicted values of TI using Equation (3) labelled "Farm" are also shown. The graph shows an initial rapid decline in measured TI with small increases in turbine separation, which then asymptotes to a near freestream value over longer distances. There is likely to be some naturally occurring variation in the freestream flow that prevents a perfect curve, but the density of turbines upstream of the nearest turbine and low event frequency for some directions also contribute to the variation. In general terms, for distances less than 13D, both models perform in a similar way—unsurprisingly as they both utilise Equation (4) for distances less than 10D. For distances greater than 13D, the more appropriate model choice appears to depend on whether TI is dissipated slower than predicted by Equation (4). It should be pointed out that the Frandsen model is a conservative model and tends in many cases to estimate levels of TI, which may be somewhat higher than those observed. From a design point of view, this may be preferable although overconservative values may lead to higher than necessary design costs. At the shortest distances (within the near wake) Equation (4) significantly overestimates the mean TI and predicts values similar to the more extreme values measured. There are three individual distances shown in Figure 13 where the measured TI is significantly greater than values predicted by either model (26.35D, 34.80D, and 35.88D). Each of these anomalies are considered to be consequences of Equation (10) defining view angles that are too narrow. For example, the most significant TI anomaly at 34.80D occurs at mast IGMMX for freestream wind directions of 50° and 51° with the nearest upstream turbine assuming Equation (10) is IGH11. However, freestream wind directions of 49° and 52° from IGMMX correspond to turbines IGG10 and IGF10 located 26.35D and 2.46D, respectively. If Equation (10) had extended the view angles of these nearer turbines each by just 1°, then this 34.8D distance would not exist in Figure 13 and the individual events would contribute to shorter distances where higher TI values are expected. Because of the large variability in differences in distance between IGMMX and the upstream turbines for this narrow sector, it is possible that turbine IGF10 would have a greater influence on TI than IGG10. Indeed, the anomaly at 26.35D in Figure 13 may also be influenced by turbulence generated by turbine IGF10, although it is noted that IGG10 corresponds to a view angle sectors of 43° to 49° as turbine IGF09's view angle sector supersedes it (distance 16.37D) for a freestream direction of 42°. As such, if Equation (10) were modified to increase view angles of closer turbines, some of the higher TI events would move left in Figure 11 to shorter turbine separations where the simplified model predicts these larger values. For comparison, the anomaly at 35.88D is the result of freestream flow from 65° with σ measured at mast IGMMZ influenced by turbine IGG02. Freestream flow from 64° and 66° at IGMMZ corresponds to turbines IGE04 and IGH02 with distances 14.41D and 45.80D, respectively. Again, if Equation (10) were modified to increase view angles of nearer turbines by just 1°, the events in this anomaly would all be relocated in Figure 13 to 14.41D and be more appropriately modelled.

4.4 | Turbulence intensity variation along a row of turbines

The Frandsen model assumes that turbulence intensity in a particular direction only depends on the proximity of the closest turbine, even if there are further turbines in the "line of sight." Furthermore, it is assumed that this turbulence intensity is only a function of the freestream wind regardless of how deep the location is in the wind farm. To test this hypothesis, two rows of turbines were examined to see how the TI varied along a row and how well this was predicted by the Frandsen and Simplified models. These two rows are marked as "Row 1" and "Row 2' in Figure 3. Figure 14 shows how TI varies along the line of turbines from IGD13 to IGD01 (Row 1) for a 10-ms^{-1} freestream wind. In this case, all but the first two turbines are closer than 10D, and so both models utilise Equations (4) and (9) at these locations whilst they differ at the second turbine (with upstream separation greater than 10D) where the Frandsen model relies on FT whilst the Simplified acknowledges the wake effect of upstream turbine IGD13. It can be seen that the Frandsen model fails to capture the increase in mean TI at the second turbine (turbine separation

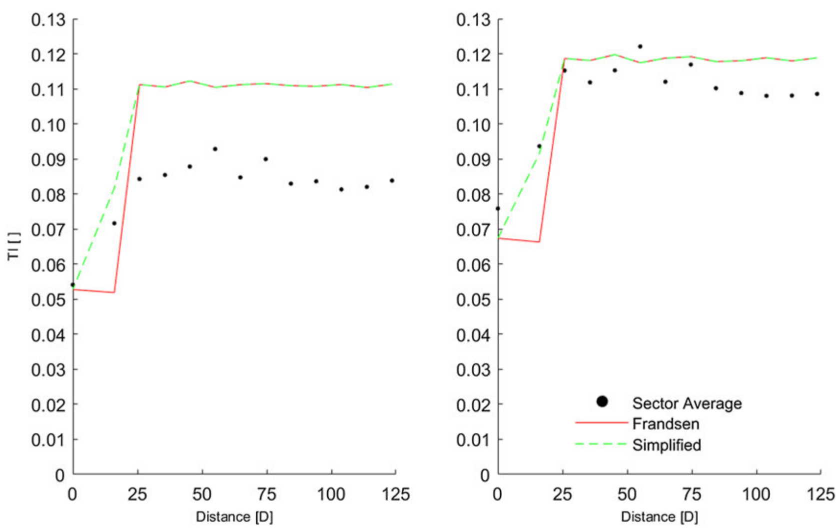

FIGURE 14 Mean (left) and representative (right) TI along the row of turbines IGD13 to IGD01 for freestream wind direction 200 ± 2° at 10 ms^{-1}. Distance is measured from the upstream turbine IGD13. Note: Large black dots (sector average) represent 10° sector averages taken from measurements [Colour figure can be viewed at wileyonlinelibrary.com]

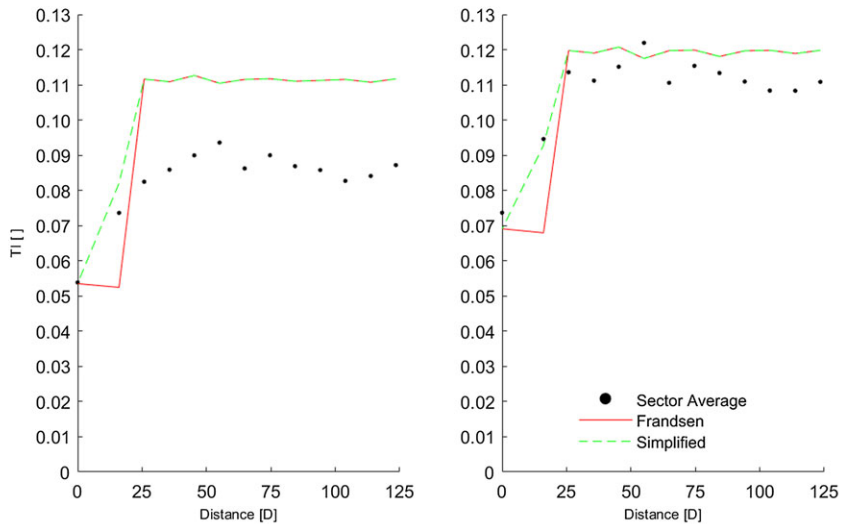

FIGURE 15 Mean (left) and representative (right) TI along the row of turbines IGF10 to IGM01 for freestream wind direction 246 ± 2° at 10 ms^{-1}. Distance is measured from the upstream turbine IGF10. Note: Large black dots (sector average) represent 10° sector averages taken from measurements [Colour figure can be viewed at wileyonlinelibrary.com]

is 16D and FT is assumed). There is a better match for the subsequent turbines, which are spaced closer than 10D although the model consistently overpredicts the mean TI down the remaining row of turbines. The Simplified model gives a good prediction for the second turbine and then matches the values returned by the Frandsen model as both use the same equation for the subsequent turbines. Both models perform better with the representative TI, although still over predicting it. However, this may be due to the partial cancellation of two errors due to overprediction of the mean turbulence and underprediction of the variance of the turbulence.

In the case of Row 2 as shown in Figure 15, all of the turbines are greater than 10D apart. The Frandsen model significantly under predicts representative TI at all locations, even when using WFT from 50.5D onwards, where ambient WFT intensity is assumed to prevail. The Simplified model by comparison generally follows the representative measured values, but there is larger variance between the turbines. However, the same comment applies as above with respect to the partial cancellation of errors. For this direction, the Simplified model overpredicts mean TI for all wake-effected turbines and neither model predicts the freestream TI measured at IGF10.There may be an effect due to the location of mast IGMMX 2.46D upstream in this direction; however, this is likely to be small.

5 | CONCLUSIONS

For the case of the Greater Gabbard offshore wind farm, the Frandsen model provides a reasonable prediction of turbulence intensity for locations in a wind farm that are deemed to be directly wake affected, although levels are somewhat overpredicted in the near wake for which the model was not really designed. It was found that switching the method of defining σ between "wake"-generated turbulence and "farm"-generated turbulence for distances beyond 10D was somewhat arbitrary and can lead to peaks in TI not observed in the data. Similarly, assuming that fewer than five turbines located more than 10D upstream will have no impact on the wind flow also leads to errors, this time the underprediction of TI. A Simplified version of the Frandsen model has been proposed, which assumes only FT or wake-generated turbulence that is not assumed to transition to WFT at some arbitrary cut-off distance. This has been shown to better predict in general turbulence intensity than the standard Frandsen model, although it is less conservative as a result.

The Frandsen model does not consider the influence of turbines beyond the closest and turbulence is assumed to depend on upstream conditions regardless of distance into the wind farm. An analysis of turbulence intensity along a row of turbines bears this out to an extent although again the assumption of "farm"-generated turbulence at the arbitrary 10D cut-off was shown to be questionable.

The observed difference in mean and representative TI is larger than that calculated by both the Frandsen and Simplified models. The assumption that variability in the FT drives the variability in the overall levels of turbulence would seem not to be entirely accurate, and it may be that there is additional variability added by the rotor-generated turbulence that needs to be accounted for. It may also be that the variance in the turbulence is not exactly Gaussian distributed meaning that the value of 1.28 in Equations (2) and (3) may not be appropriate. This requires further investigation.

Furthermore, from data at both masts, a comparison between measured and modelled TI vs turbine distance showed a good agreement between data and model, with only a few outliers. An investigation about the cause for the outliers suggests that these could all be removed if the view angle proposed by Frandsen is increased slightly. It is not clear whether this is true in general, or whether this is site specific. It should also be pointed out that as the Frandsen model seems to overestimate TI for turbines closer than 10D, increasing the view angle might on average produce even more conservative estimates of the effective TI. The intention of this research was to assess the Frandsen model as proposed although further work should be performed to assess the sensitivity of the model to various parameters including the view angle.

It should be pointed out that there are a number of caveats to the conclusions above. The findings are based on only a limited number of turbines in one large offshore wind farm. A much broader range of turbines should be analysed for a number of such wind farms to provide definitive conclusions. In addition, it is well known that there are limitations in using nacelle-mounted anemometry for the determination of accurate wind speed, wind direction, and turbulence intensity measurements. Nonetheless, the results of this work should provide a valuable insight into the applicability of the Frandsen model in a large offshore wind farm array.

ACKNOWLEDGEMENTS

This work was funded by the Offshore Wind Accelerator (OWA) project of the Carbon Trust, and data were provided by Scottish and Southern Energy (SSE). The authors would like to thank the OWA partners and the Carbon Trust for many valuable and stimulating discussions on the work, especially Ørsted (formerly DONG Energy) and Paul Housley of SSE. The authors would particularly like to thank Cameron Brown of Ørsted for useful discussions and access to results with regard to the validity of the Frandsen model when assuming WFT.

ORCID

Simon Watson http://orcid.org/0000-0001-6694-3149

REFERENCES

1. Frandsen S. Turbulence and turbulence generated loading in wind turbine clusters. *RISO Rep*. 2007;R-1188.
2. Gottschall J, Peinke J. How to improve the estimation of power curves for wind turbines. *Environ Res Lett*. 2008;3(1):015005.
3. IEC Standard, 61400–1, Edition 3 + amendment 1, 2010. Wind turbines, Part 1: design requirements, BS EN 61400–1:2005 + A1:2010.
4. Schlez W, Neubert A. New developments in large wind farm modelling. In: *European Wind Energy Conference*. Marseille; 2009.
5. Aubrun S, Loyer S, Espana G, Hayden P, Hancock P. Experimental study on the wind turbine wake meandering with the help of a non-rotation simplified model and of a rotating model. In: *49th AIAA Aerospace Sciences Meeting Including the New Horizons Forum and Aerospace Exposition*. Orlando; 2011.
6. Jacquemin J, Traylor H, Muir N, Cordle A, Baldock N, Devaney L. Effective turbulence calculations using IEC 61400-1 edition 3: Reaching consensus through dialogue and action. In: *European Wind Energy Association Conference and Exhibition*. Warsaw; 2010.
7. Crespo A, Hernández J. Turbulence characteristics in wind-turbine wakes. *J Wind Eng Ind Aerodyn*. 1996;61(1):71-85.
8. Stevens RJAM, Meneveau C. Flow structure and turbulence in wind farms. *Annu Rev Fluid Mech*. 2017;49(1):311-339.
9. Frandsen S, Madsen PH. Spatially average of turbulence intensity inside large wind turbine arrays. In: *Proceedings of the European Seminar Offshore Wind Energy in Mediterranean and Other European Seas*, 10th – 12th April. Naples, Italy; 2003:97-106.
10. Barthelmie RJ, Frandsen SM, Nielsen MN, Pryor SC, Rethore P-E, Jørgensen HE. Modelling and measurements of power losses and turbulence intensity in wind turbine wakes at Middelgrunden offshore wind farm. *Wind Energy*. 2007;10:517-528.
11. Brand A, Wagenaar J-W. Turbulent wind turbine wakes in a wind farm. In: *Progress in Turbulence and Wind Energy IV: Proceedings of the iTi Conference in Turbulence*. Bertinoro, Italy; 2010:2010.
12. Larsen G. *From Solitary Wakes to Wind Farm Wind Fields—A Simple Engineering Approach*. Roskilde, Denmark: DTU Wind Energy; 2009.
13. Chamorro LP, Porté-Agel F. Turbulent flow inside and above a wind farm: a wind-tunnel study. *Energies*. 2011;4(11):1916-1936.
14. Chamorro LP, Arndt REA, Sotiropoulos F. Turbulent flow properties around a staggered wind farm. *Bound-Lay Meteorol*. 2011;141(3):349-367.
15. Markfort C, Zhang W, Porté-Agel F. Turbulent flow and scalar transport through and over aligned and staggered wind farms. *J Turbul*. 2012;13(33):1-36.
16. Göçmen T, Giebel G. Estimation of turbulence intensity using rotor effective wind speed in Lillgrund and horns rev-I offshore wind farms. *Renew Energy*. 2016;99:524-532.
17. Andersen SJ, Sørensen JA, Mikkelsen R, Ivanell S. Statistics of LES simulations of large wind farms. *J Phys Conf Ser*. 2016;753:032002.
18. Larsen TJ, Madsen MA, Larsen GC, Hansen KS. Validation of the dynamic wake meander model for loads and power production in the Egmond aan Zee wind farm. *Wind Energy*. 2013;16(4):605-624.

How to cite this article: Argyle P, Watson S, Montavon C, Jones I, Smith M. Modelling turbulence intensity within a large offshore wind farm. *Wind Energy*. 2018;21:1329–1343. https://doi.org/10.1002/we.2257